



# Flexural and shear strengthening of RC beams with composite materials – The influence of cutting steel stirrups to install CFRP strips

Inês G. Costa, Joaquim A.O. Barros \*

Department of Civil Engineering, University of Minho, 4800-058 Guimarães, Portugal

## ARTICLE INFO

### Article history:

Received 20 April 2009

Received in revised form 4 March 2010

Accepted 5 March 2010

Available online 12 March 2010

### Keywords:

CFRP

NSM

Flexural strengthening

Shear strengthening

Stirrups

## ABSTRACT

Experimental, numerical and analytical investigations have revealed that Carbon Fibre Reinforced Polymer (CFRP) strips with larger cross section height improve the effectiveness of the Near Surface Mounted (NSM) technique for the flexural strengthening of existing reinforced concrete (RC) beams. However, this height is limited to the concrete cover thickness of the longitudinal steel bars, since the application of strips of cross section height larger than the cover thickness requires that the bottom arm of the steel stirrups be cut. This work aims to assess the influence, in terms of shear resistance, of cutting the bottom arm of steel stirrups to install NSM strips for the flexural strengthening of RC beams. The obtained results showed that, for monotonic loading, cutting the bottom arm of steel stirrups led to a decrease of the beam's load carrying capacity of less than 10%. Due to the high effectiveness of the adopted NSM flexural strengthening systems, shear can be a predominant failure mode for these beams. To avoid this type of failure mode, strips of wet lay-up CFRP sheets with U configuration were used, resulting in effective strengthening solutions for RC beams. In the present paper the experimental program is described, and the obtained results are presented and discussed.

© 2010 Elsevier Ltd. All rights reserved.

## 1. Introduction

Sustainable rehabilitation practices require the use of competitive strengthening solutions. The techniques based on the use of Carbon Fibre Reinforced Polymer (CFRP) strips and wet lay-up sheets can be very competitive, since CFRP materials have high mechanical and durability performance, are lightweight, easy to install, and do not change significantly the original geometry of the strengthened elements. The Externally Bonded Reinforcement (EBR) [1] and the Near Surface Mounted (NSM) [2,3] techniques are most commonly used for the strengthening of reinforced concrete (RC) elements.

The NSM technique consists of installing CFRP strips into thin slits opened on the concrete cover of the elements to strengthen. The strips are bonded to the surrounding concrete by using an epoxy-based adhesive. FRP bars of round or square cross section made of carbon, glass or aramid fibres have been used in the NSM technique [4,5], but available experimental [6], analytical and numerical [7] research demonstrates that strips of rectangular cross section are the most effective in terms of strengthening performance. Using the NSM technique, significant flexural strengthening effectiveness was obtained for beams [8], slabs [9], as well as in terms of the shear strengthening of RC beams [10].

Significant increments in terms of flexural and shear resistance can also be achieved with the EBR technique but, when compared to the strengthening effectiveness provided by the NSM technique, EBR is not as competitive, due to its longer execution times and susceptibilities to acts of vandalism and to the effects of environmental aggressiveness [3]. To take into account the occurrence of FRP premature debonding failure modes, the FRP design tensile strain should be limited to a certain value [1] that can be significantly lower than its ultimate tensile strain value obtained in tensile tests with FRP specimens, which is a serious concern for the competitiveness of FRP-based strengthening techniques.

Experimental [11], numerical and analytical [7] studies have also shown that the larger is the height of the CFRP strip cross section the more effective is the NSM flexural strengthening. However, this height is limited to the thickness of the concrete cover, since the use of strips with a cross section height larger than the concrete cover thickness requires that the bottom arm of the steel stirrups be cut.

The influence, in terms of the beam's load carrying capacity, of cutting the bottom arm of steel stirrups for the installation of CFRP strips is analysed in the present work. To take into account relevant aspects for this study, the experimental program is composed of beams of distinct cross section depth, since it is reasonable to assume that the deeper is the beam cross section the smaller might be the influence of cutting the bottom arm of the stirrups in terms of the NSM flexural strengthening effectiveness.

\* Corresponding author. Tel.: +351 253510210; fax: +351 253510217.

E-mail address: [barros@civil.uminho.pt](mailto:barros@civil.uminho.pt) (J.A.O. Barros).

## Nomenclature

$E_c$	modulus of elasticity of concrete (at 28 days)	$f_{fu}^*$	tensile strength of the FRP
$E_f$	modulus of elasticity of FRP	$f_{sum}$	steel tensile strength
$E_{sm}$	modulus of elasticity of steel	$f_{sym}$	steel yield strength
$E_{sm,eq}$	equivalent modulus of elasticity of steel = $(\sum E_{sm,i} \times A_{si}) / (\sum A_{si})$	$f_{sym,eq}$	equivalent steel yield strength = $(\sum f_{sym,i} \times A_{si}) / (\sum A_{si})$
$F_{max}$	maximum experimental load	$tf$	thickness of FRP
$F_{Rd}$	design resistant load	$\epsilon_{fu}^*$	ultimate FRP strain
$F_{sy}$	yield initiation load (at $\epsilon_{sy,eq}$ )	$\epsilon_{fL,Fmax}$	strain in the strips at $F_{max}$
$F_{VEi}$	maximum experimental load obtained testing VEi	$\epsilon_{fL,max}$	maximum strain in the strips
$F_{VRi}$	maximum experimental load obtained testing VRi	$\epsilon_{fV,Fmax}$	strain in the strips of wet lay-up CFRP sheets at $F_{max}$
$f_{ck}$	characteristic value of the concrete compressive strength	$\epsilon_{fV,max}$	maximum strain in the strips of wet lay-up CFRP sheets
		$\epsilon_{sy,eq}$	equivalent steel yield strain ( $f_{sym,eq}/E_{sm,eq}$ )

A relatively high strengthening ratio of CFRP strips was used in order to promote the occurrence of shear failure mode for the strengthened beams. To avoid the occurrence of this brittle and abrupt failure mode, the beams strengthened in flexure were also strengthened in shear using strips of wet lay-up CFRP sheets of U configuration that were placed between existing steel stirrups. The experimental program is described and the results are presented and discussed.

## 2. Characteristics of the beams and strengthening systems

The experimental program is composed of three series of beams. Each series differs in cross section height and contains four beams (Fig. 1 and Table 1). For the generic  $i$ th series the beams have the following designations:

- VRi – reinforced concrete reference beam.
- VEi – equivalent to the VRi beam, but with the bottom arm of the steel stirrups cut.
- VLi – equivalent to the VEi beam, and strengthened in flexure with NSM CFRP strips.
- VLMi – equivalent to the VLi beam, and strengthened in shear with strips of wet lay-up CFRP sheets of U configuration.

All beams have a cross section width ( $b$ ) of 0.2 m in order to assure the same anchorage length to the bottom arm of the steel stirrups.

The percentage of NSM CFRP strips applied in the VLi and VLMi beams of the  $i$ th series was designed in order to have the potential of doubling the load carrying capacity of the corresponding VRi reference beam. However, this strengthening capacity can be compro-

mised in beams without shear strengthening systems, since the VLi beams have a shear resistance lower than the flexural capacity that NSM CFRP strips can provide. This justifies the presence of VLMi beams in the tested series, with a hybrid strengthening configuration in an attempt to avoid the occurrence of shear failure modes. The EBR U shear strengthening configuration of wet lay-up CFRP sheets has also the purpose of offering extra resistance to an eventual premature detachment of the NSM strips in the tested region of the beams (smaller shear span).

For the flexural strengthening of a beam, two CFRP strips of 1.4 mm × 20 mm cross section dimensions were used (Fig. 2). Since the *fib* bulletin 14 [12] does not have recommendations for the flexural strengthening design with NSM systems, the ACI 440 [1] recommendations were followed. However, for the design of the shear strengthening configurations the *fib* guidelines [12] were adopted, and three strips of one layer of wet lay-up CFRP sheet of 50 mm width ( $w_f$ ) were obtained, which were placed according to the scheme represented in Fig. 2.

The strengthening systems were applied in order to reproduce, as much as possible, the conditions found on a job site. Therefore, the extremities of the strips remained 100 mm far from the supports of the beams, since due to the intrinsic process of opening the slits in real RC frames (see Fig. 3) they can not be opened up to the faces of the supporting RC columns.

With the same concern, a U configuration for the shear strengthening systems was adopted, since a full wrapping shear configuration, despite being the most effective shear strengthening strategy [13], rarely can be applied, due to the continuous character of the beam/slab connection.

In the three series of beams the shear span ratio ( $L_1/d$ , where  $d$  is the internal arm of the cross section) was maintained almost constant and equal to 2.5. This value favours the occurrence of shear failure mode in the beams strengthened in flexure. The three series of beams have cross section of distinct height in order to provide different bond transfer length for the stirrups and for the CFRP strips of wet lay-up sheet crossed by the shear failure crack, since this parameter is highly relevant in terms of shear strengthening effectiveness. To localize the occurrence of the shear failure crack in the  $L_1$  span of the strengthened beams (Fig. 1), this span has a smaller length than the  $L_2$  span in all the tested beams.

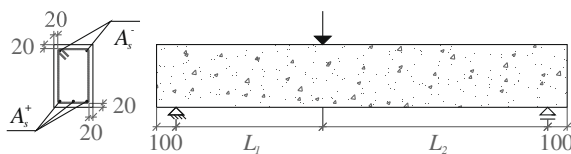


Fig. 1. Beam geometry and loading conditions – see Table 1 (dimensions in mm).

Table 1  
Dimensions of the beams of the three series.

Series	$L_1$ (mm)	$L_2$ (mm)	$b$ (mm)	$h$ (mm)	$A_s^+$ (bottom face)	$A_s^-$ (top face)
1	550	950	200	250	$2\phi 10 + 1\phi 6$	$2\phi 10$
2	750	1150	200	320	$2\phi 10 + 1\phi 10$	$2\phi 10$
3	900	1300	200	380	$2\phi 12 + 1\phi 8$	$2\phi 12$

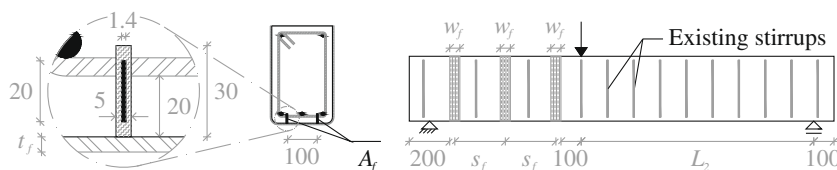


Fig. 2. Representation of the flexural and shear strengthening systems (dimensions in mm).

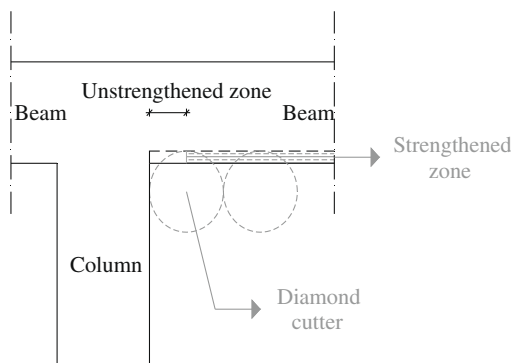


Fig. 3. NSM flexural strengthening in job site real conditions.

Table 2  
Concrete properties.

Property	In pre-design phase	Experimental characterization
$f_{cm}$ (MPa)	20.0	31.1
$E_c$ (MPa)	29.0	28.9

Table 3  
Steel properties.

Property	In pre-design phase	Experimental characterization			
		$\phi$ 6	$\phi$ 8	$\phi$ 10	$\phi$ 12
$f_{sym}$ (MPa)	400	571	546	548	597
$f_{sum}$ (MPa)	–	662	653	648	738
$E_{sm}$ (GPa)	200	166	173	174	202

Table 4  
Properties of CFRP strips and sheets.

Property	According to the supplier		Experimental characterization	
	CFK laminate	C sheet 240	CFK laminate	C sheet 240
$f_{tu}^*$ (MPa)	1850	3800	2783	3257
$E_f$ (GPa)	165	240	157	237
$\epsilon_{fu}^*$ (‰)	11.2	15.83	17.8	13.77
$t_f$ (mm)	1.4	0.117	1.42	0.117
Adhesive	S&P resin 220	S&P resin 50/55	S&P resin 220	S&P resin 50/55

### 3. Material properties and monitoring system

#### 3.1. Materials

In the pre-design phase of the beams, the values assumed for the properties of the intervening materials are included in Tables 2–4. The corresponding values obtained in experimental tests are also included in these tables. The meaning of the symbols in these tables is indicated in Nomenclature. In Table 4 the CFK Laminates represent the CFRP strips applied with the NSM technique for the

flexural strengthening of the RC beams, while the strips of U configuration adopted to increase the shear resistance of the VLMi beams were made from the C Sheet 240.

#### 3.2. Monitoring system

##### 3.2.1. Strain gauges

In each beam, two strain gauges were applied in the steel stirrup ( $SG_{SV}$ ) that was assumed as being the most stressed at the moment of the formation of the shear failure crack. The position of the  $SG_{SV}$  is indicated in Fig. 4a. In each beam, at the loaded section, a strain gauge ( $SG_{SL}$ ) was applied in one longitudinal steel bar, as represented in Fig. 4a. In both CFRP strips of the strengthened beams, at the loaded section, one strain gauge ( $SG_{CL}$ ) was applied, as represented in Fig. 4b.

In the beams strengthened in shear, three strain gauges were installed on the intermediate strip of wet lay-up CFRP sheet, according to the representation indicated in Fig. 4c.

##### 3.2.2. Displacement transducers

In each test, five displacement transducers (LVDTs) were placed according to the disposition indicated in Fig. 5. The LVDTs were supported on an aluminium bar fixed in the alignments of the supports of the beam in order to avoid extraneous readings, like beam support settlements and deformability of the test reaction frame.

### 4. Experimental results

#### 4.1. Series 1 beams

The behaviours of the VR1 and VE1 beams were almost the same, both in terms of load carrying capacity and in crack pattern (Figs. 6 and 11). Both beams failed in bending, with the steel yield initiation at about 2.5 mm beam deflection, for a load of 58 kN.

In spite of having supported a load level significantly higher than its VR1 reference beam, the potential duplication of the load carrying capacity that NSM strips applied in VL1 beam could provide was not attained due to the occurrence of a shear failure mode in VL1 beam, as expected. However, it is quite notable that, at the moment of the shear failure, the longitudinal steel bars were already yielded in all the beams of Series 1 (Fig. 7). In fact, the longitudinal steel bars started yielding at a beam deflection of 3.3 mm, for a load of 79 kN when the maximum strain in the CFRP strips was 3.2‰ (Fig. 9).

When compared with the VR1 and VE1 beams, VL1 and VLM1 beams presented a higher stiffness after crack initiation. However, the behaviour of VLM1 beam shows that the applied shear strengthening system had marginal contribute to the beam's stiffness.

Due to a premature debonding of the shear strips crossed by the shear failure crack, VLM1 beam also failed in shear, which was not expected. The longitudinal steel bars of VLM1 beam started yielding at a beam deflection of 3.2 mm, for a load of 79 kN, when the maximum strain in the CFRP strips was 3.2‰ (Fig. 7).

Fig. 7 and the results included in Table 5 show that cutting the bottom arm of the steel stirrups had no influence on the load

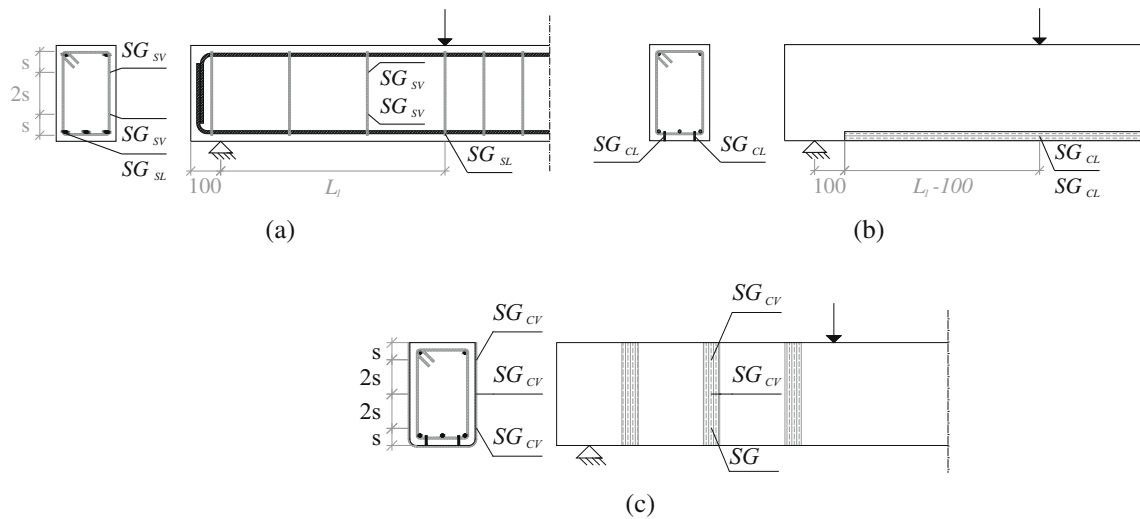


**Fig. 4.** Locations of the strain gauges (SG) installed on: (a) a steel stirrup ( $SG_{sv}$ ) and on a longitudinal steel bar ( $SG_{sl}$ ); (b) the CFRP strips ( $SG_{cl}$ ); (c) the strip of wet lay-up CFRP sheet ( $SG_{cv}$ ) (dimensions in mm).

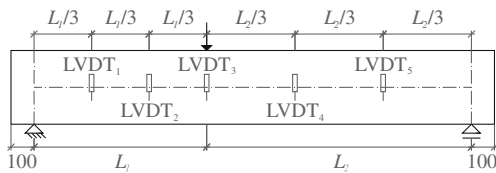


**Fig. 5.** Locations of the displacement transducers (dimensions in mm).

carrying capacity of the beams of Series 1, and that two NSM strips ( $\rho_f = 0.12\%$ ) provided an increase of about 40% in terms of beam load carrying capacity. In the 2nd, 3rd and 4th columns of Table 5 (and the same in Tables 6 and 7) are indicated the age of the beams (in days) when the beams were tested, the NSM CFRP strips were applied and the strips of wet lay-up sheet were bonded, respectively.

In spite of the VLM1 beam failing in shear, Table 5 shows that the shear strengthening configuration adopted in this beam allowed an increase of about 80% in terms of beam load carrying capacity. Therefore, if shear failure had not occurred, it would have been expectable that the NSM flexural system had doubled the load carrying capacity of the VR1 beam. In Table 5  $F_{Rd}$  is the maximum load obtained analytically using the values of the properties of the intervening materials indicated in Tables 2–4 in the column corresponding to “pre-design phase” (more details can be found

elsewhere [14]). Since the values of the characterized properties of the intervening materials were higher than those assumed in the “pre-design phase”, the values of  $F_{Rd}$  were lower than those registered experimentally.

The photo in Fig. 8 shows the formation of a crack at the extremity of the NSM strips, and its propagation at the interface between longitudinal steel bars and concrete cover. Due to the shear sliding of the faces of the shear crack, dowel-effect occurred in the longitudinal steel bars, contributing to the detachment of the concrete cover.

Fig. 9 compares the evolution of the strains in the NSM strips (average of the two monitored strips) and in the longitudinal steel bars for the VL1 and VLM1 beams. It can be concluded that, up to the yielding of the longitudinal steel bars the variation of the strains in steel bars and CFRP strips was similar, revealing a perfect bond conditions between these strips and surrounding concrete. It is also visible that the shear strengthening system allowed the mobilization of a maximum strain of 10.0‰ in the NSM strips, which is 56% of the ultimate strain registered experimentally in this material (Table 4), while in VL1 beam the occurrence of the shear failure mode limited the maximum strain in the NSM strips to 6.4‰.

The variation of the strains in the intermediate strip of CFRP sheet of VLM1 beam is shown in Fig. 10. At about 70 kN, this strip was crossed by the shear failure crack, leading to an abrupt increase and similar variation of strains in  $SG_{cv2}$  and  $SG_{cv3}$ , while the strain

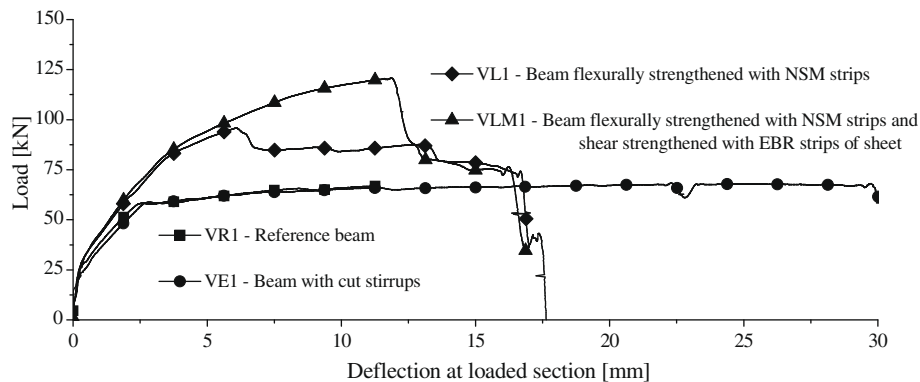


**Fig. 6.** Deflection-load relationship for the beams of Series 1.

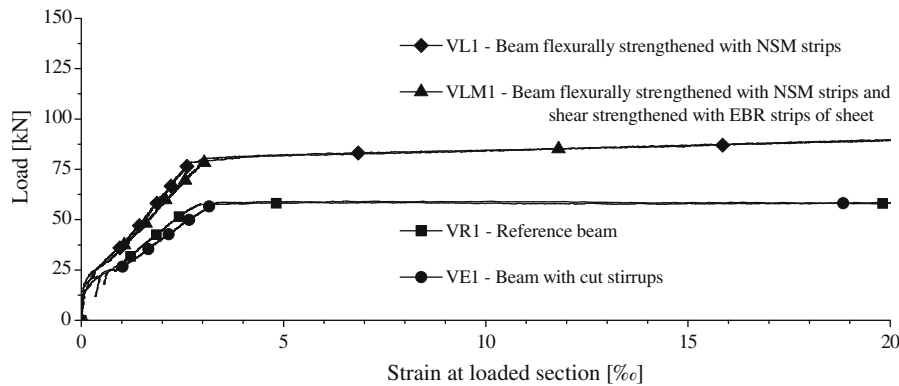


Fig. 7. Relationship between the strains in the longitudinal steel bars ( $SG_{SL1}$ ) and the applied load.

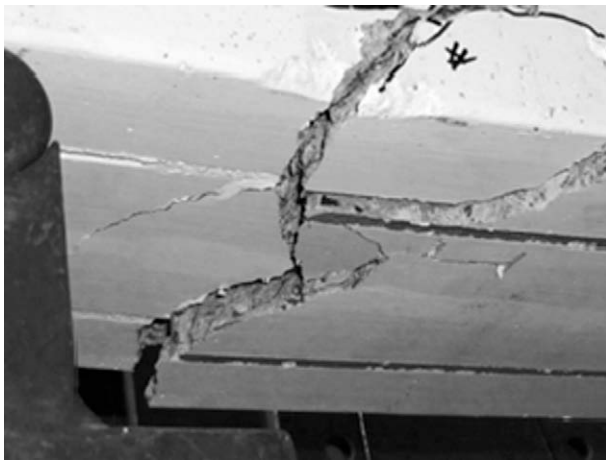


Fig. 8. Detail of the zone of the extremity of the strips at beam's failure.

variation in  $SG_{CV1}$  was very small, in consequence of being quite far from the shear crack plane and also due to a premature debonding at the free extremity of this strip. It is quite significant the 7.53‰ maximum strain at  $SG_{CV3}$ , which is a little lower than the average value adopted in the design of the CFRP shear strengthening systems ( $\epsilon_{fe} = 8.5\%$ , according to fib bulletin 14 [12]).

#### 4.2. Series 2 beams

Like in Series 1, the behaviours of the VR2 and VE2 beams of Series 2 were similar, showing that cutting the bottom arm of the stirrups did not influence the load carrying capacity of the

tested beams. In similitude to what occurred in Series 1, VL2 beam of Series 2 also failed in shear. However, the inclination of the shear failure crack of VL2 beam was lower than the one of VL1 beam. Furthermore, the shear failure crack of the VL1 beam has an almost constant inclination, while in the VL2 beam the inclination of the shear failure crack changed significantly along its development (Fig. 11a and b).

In the test of VLM2 beam, along the  $L_2$  span (Fig. 2), the strips together with the surrounding concrete were detached (Fig. 11c), which indicates that the shear strengthening system was effective in terms of avoiding the occurrence of shear failure in the  $L_1$  beam's span. This means that the total resisting bond length of the strips of sheet provided enough resistance in order to avoid the degeneration of the existing shear cracks into a shear failure crack.

Fig. 12 shows that in the bottom tensile face along the  $L_2$  of VLM2 beam's span, a fish spine crack pattern was formed, in consequence of the stress transfer between strips and surrounding concrete [8,9]. In general, this crack pattern occurs when high stress levels are installed in the strips, which is an indicator of the high performance of the used adhesive in terms of strip-concrete bond behaviour. In fact, the maximum strain measured in the CFRP strips in VLM2 beam was 12.3‰ (Table 6).

The relationship between the applied load and the deflection at the loaded beam section is represented in Fig. 13 for the four beams of Series 2. Table 6 includes the most significant results obtained the tests of this series. From Table 6 it is visible that the increase in terms of beam's load carrying capacity provided by the strengthening of two laminates ( $\rho_f = 0.090\%$ ) was 55%, while combining the flexural and shear strengthening systems (VLM2) assured an increase of about 77%. It is also observed that the loss of load carrying capacity due to the cut of the bottom arm of the stirrups was again very small.

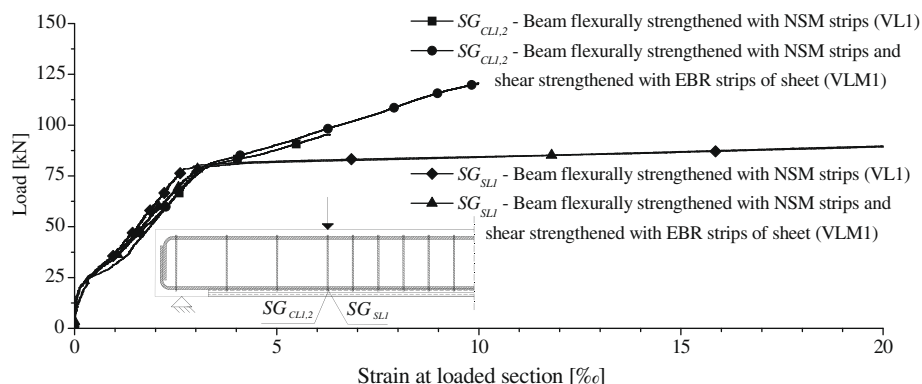


Fig. 9. Relationship between the applied load and the strains in both the longitudinal steel bars ( $SG_{SL1}$ ) and NSM strips ( $SG_{CL1,2}$ ).



**Table 5**

Results from the beams of Series 1.

Beam	Age at testing beams (days)			$F_{Rd}$ (kN)	$F_{sy}$ (kN)	$F_{max}$ (kN)	$\frac{F_{max}}{F_{VR1}}$	$\frac{F_{max}}{F_{VE1}}$	$\varepsilon_{fl,Fmax}$ (‰)	$\varepsilon_{fl,Fmax}$ (‰)	$\varepsilon_{IV,max}$ (‰)	$\varepsilon_{IV,max}$ (‰)
	RC	NSM	EBR									
VR1	35	–	–	38	58	67	1.00	0.98	–	–	–	–
VE1	37	–	–	38	57	69	1.02	1.00	–	–	–	–
VL1	50	14	–	71	79	96	1.43	1.40	6.4	6.4	–	–
VLM1	67	31	9	71	79	121	1.80	1.76	10.0	10.0	6.2	7.5

Note:  $F_{sym,eq}$  = 552 MPa;  $E_{sm,eq}$  = 173 GPa;  $\varepsilon_{sy,eq}$  = 3.2‰.**Table 6**

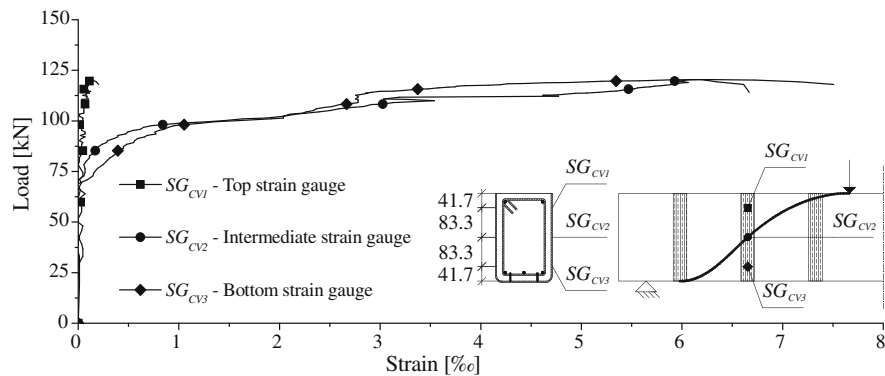
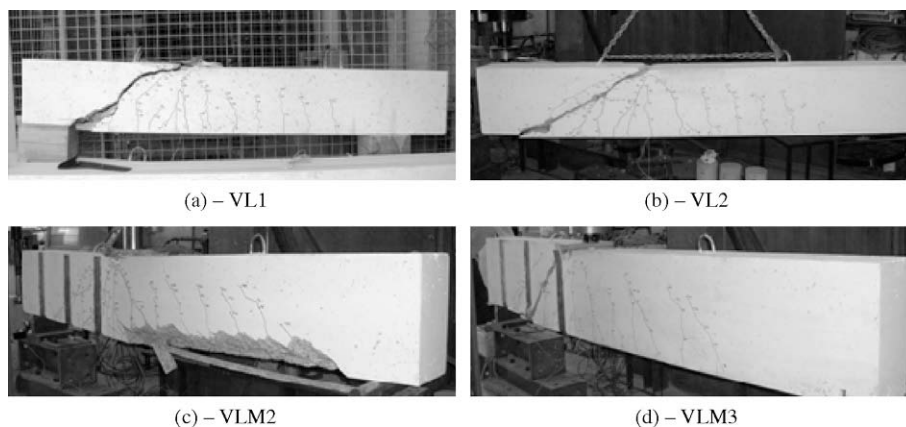
Results from the beams of Series 2.

Beam	Age at testing beams (days)			$F_{Rd}$ (kN)	$F_{sy}$ (kN)	$F_{max}$ (kN)	$\frac{F_{max}}{F_{VR2}}$	$\frac{F_{max}}{F_{VE2}}$	$\varepsilon_{fl,Fmax}$ (‰)	$\varepsilon_{fl,Fmax}$ (‰)	$\varepsilon_{IV,max}$ (‰)	$\varepsilon_{IV,max}$ (‰)
	RC	NSM	EBR									
VR2	38	–	–	49	70	88	1.00	1.00	–	–	–	–
VE2	37	–	–	49	–	89	1.00	1.00	–	–	–	–
VL2	51	9	–	85	87	137	1.55	1.55	9.6	9.6	–	–
VLM2	66	24	8	85	–	156	1.77	1.76	12.3	12.3	3.9	4.0

Note:  $F_{sym,eq}$  = 548 MPa;  $E_{sm,eq}$  = 174 GPa;  $\varepsilon_{sy,eq}$  = 2.6‰.**Table 7**

Results from the beams of Series 3.

Beam	Age at testing beams (days)			$F_{Rd}$ (kN)	$F_{sy}$ (kN)	$F_{max}$ (kN)	$\frac{F_{max}}{F_{VR3}}$	$\frac{F_{max}}{F_{VE3}}$	$\varepsilon_{fl,Fmax}$ (‰)	$\varepsilon_{fl,Fmax}$ (‰)	$\varepsilon_{IV,Fmax}$ (‰)	$\varepsilon_{IV,Fmax}$ (‰)
	RC	NSM	EBR									
VR3	53	–	–	59	90	116.03	1.00	1.12	–	–	–	–
VE3	53	–	–	59	85	103.26	0.89	1.00	–	–	–	–
VL3	58	8	–	98	107	148.28	1.28	1.44	7.6	7.7	–	–
VLM3	65	14	7	98	112	157.96	1.36	1.53	10.0	10.1	5.0	9.5

Note:  $F_{sym,eq}$  = 557 MPa;  $E_{sm,eq}$  = 197 GPa;  $\varepsilon_{sy,eq}$  = 2.8‰.**Fig. 10.** Relationship between the strains in the EBR strip of sheet ( $SG_{CV1}$ ,  $SG_{CV2}$ ,  $SG_{CV3}$ ) and the applied load, in VLM1 beam (dimensions in mm).**Fig. 11.** Crack patterns at the end of the tests of the beams: (a) VL1, (b) VL2, (c) VLM2, (d) VLM3.

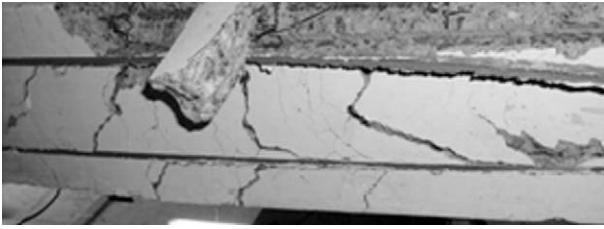


**Fig. 12.** Crack pattern of the bottom surface of the VLM2 beam along the  $L_2$  span, at the end of the test.

Similar to what happened in the beams of Series 1, when the beams of Series 2 failed, their longitudinal steel bars had already yielded. Furthermore, when shear failure crack formed in VL2 beam the longitudinal steel bars had already yielded (Fig. 13).

In terms of strain fields in steel longitudinal bars and NSM CFRP strips, they were similar to those measured in the homologous beams of Series 1.

On the other hand, the strain field registered by the strain gauges installed on the strip of sheet of VLM2 beam (Fig. 14) was distinct of the one recorded in VLM1 (Fig. 10). Since in VLM2 beam a shear failure crack was not formed in the  $L_1$  span where EBR strips of sheet were applied, the maximum strains registered in the monitored strip were lower than the corresponding ones measured in the strip of sheet of VLM1 beam.

#### 4.3. Series 3 beams

As for the VRi and VEi beams of Series 1 and 2, the VR3 and VE3 beams of Series 3 also failed in bending. However, while in Series 1 and 2 the decrease of load carrying capacity due to the cutting of the bottom arm of the steel stirrups was marginal, in the VE3 beam the decrease was higher, around 10%. This distinct behaviour may, however, not be totally related to the cutting of the steel stirrups, since a small inaccuracy in the positioning of the tensile longitudinal steel bars, or some heterogeneity on the material properties of the steel bars or concrete quality of the beams can justify this difference.

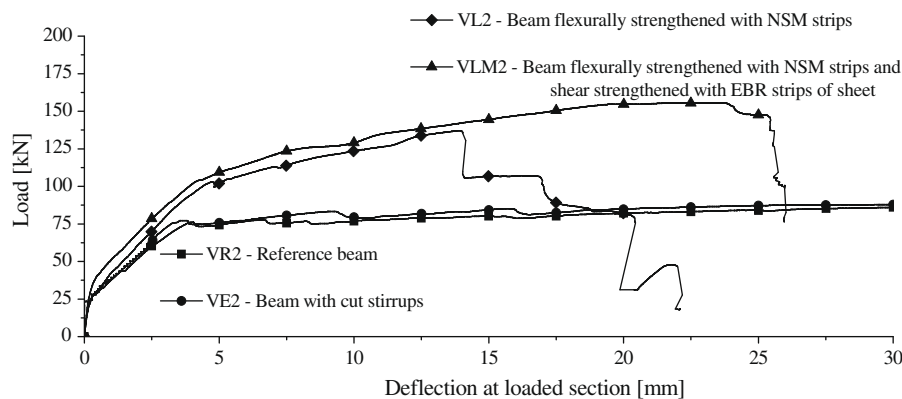


**Fig. 13.** Deflection-load relationship for the beams of Series 2.

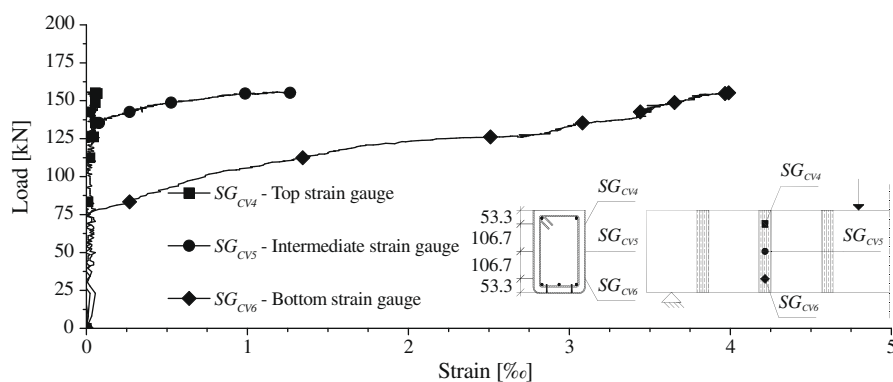


**Fig. 14.** Relationship between the strains in the EBR strip of sheet ( $SG_{CV4}$ ,  $SG_{CV5}$ ,  $SG_{CV6}$ ) and the applied load, in VLM2 beam (dimensions in mm).

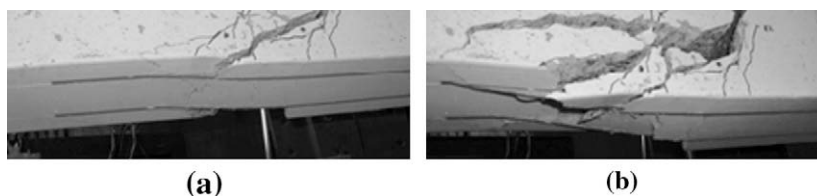


**Fig. 15.** Evolution of the expulsion of the strips of VL3 beam.

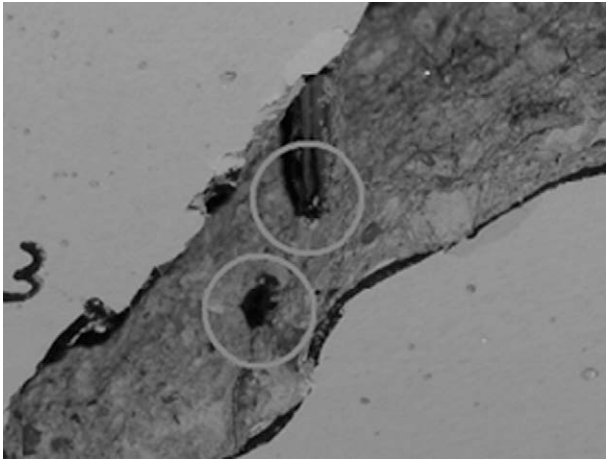


Fig. 16. Failure of the stirrup closest of the loaded section (VL3 beam).



Fig. 17. Sliding of the central stirrup in the  $L_1$  span (VL3 beam).



Fig. 18. Appearance of the NSM strips at the end of the test.

The behaviour of VL3 beam was similar to the homologous beams of the previous series, having failed in shear. The sliding of the faces of the shear failure crack had a significant influence on the detachment of the concrete cover layer involving the strips (Fig. 15) which led to a premature loss of the potential strengthening of the NSM CFRP strips. The higher cross sectional area of tensile longitudinal bars, and the larger diameter of these bars, when compared to the reinforcements used in the beams of the previous series, promoted the dowel-effect, which contributed for the detachment of the concrete cover. However, in the VL3 beam, the sliding of the faces of the shear crack did not conduct to an abrupt detachment of the extremities of the strips, as happened in the corresponding beam of the previous series. In fact, in VL3 beam the strips were progressively expelled from their slits (Fig. 15).

Fig. 16 shows that the steel stirrup of the VL3 beam, closest of the loaded section in the  $L_1$  span, has ruptured, while the other stirrups loss their capability of embracing the longitudinal steel bars (Fig. 17). This suggests that if beams with bottom arm steel stirrups cut for the installation of NSM strips are subjected to cyclic loadings, such as in the case of a seismic occurrence, the steel stirrups can lose their capacity to provide shear resistance. In fact, in this case the applicability of the truss Mörsh approach, currently used for the evaluation of the contribution of tie stirrups and concrete compressive struts for the shear resistance of RC beams, is no longer applicable. Furthermore, concrete confinement might be also affected, which can have a detrimental effect, mainly when beams are also subjected to axial compressive force. These concerns advise additional research in the behaviour of RC beams with cut steel stirrups for the installation of NSM strips, subjected to cyclic loadings. The influence of fatigue loadings should also be investigated, since the load repetitions can significantly decrease the anchorage conditions of the cut arm branches of the stirrups, with the consequent adverse repercussions in terms of shear resistance and concrete confinement that steel stirrups can guaranty.

At the end of the test, when analysing a detached concrete fragment, a portion of adhesive not completely cured at the bottom of the slit was found. This indicates that when using deeper slits for the installation of strips of relatively high cross section height, larger periods of time for the curing process of the adhesive might be necessary. It should be also reported the occurrence of longitudinal failure lines along the CFRP strips of VL3 beam (Fig. 18), in consequence of the curvature applied to the strips during the process of their “expulsion” from the interior of the slits (Fig. 15).

When designing the CFRP shear strengthening system for VLM3 beam, the recommendation [12] for a distance between consecutive strips of sheet ( $s_f$ , Fig. 2) less than  $0.9d_s - w_f/2$  ( $w_f$  is the width of the strip of sheet,  $d_s$  is the effective depth of the beam's cross section,  $s_f = 296$  mm) was disregarded. In this beam the distance between strips of sheet ( $s_f = 325$  mm) was higher than the maximum value of  $s_f$  recommended by [12], which contributed for the occurrence of a shear failure mode (Fig. 19).

From Table 7 and Fig. 19 it is verified that the increase in term of load carrying capacity provided by two NSM CFRP strips applied in VL3 beam ( $\rho_f = 0.076\%$ ) was 28%, while the flexural and shear strengthening strategy adopted in VLM3 beam allowed an increase of 36%. The results in this table also show that cutting the bottom arm of the steel stirrups of the beam of this series led to a decrease of 11% in terms of beam's load carrying capacity. Although VLM3 beam has failed in shear, at the maximum load the strain on the CFRP strip was 10‰, which is 56% of the material ultimate strain, similar to the value recorded in the corresponding beam of Series 1. The strain fields in the longitudinal steel bars and NSM CFRP strips were similar to those measured in the homologous beams of the previous series.

The relationship between the applied load and the strains recorded in the strain gauges applied in the intermediate strip of sheet is depicted in Fig. 20. In this beam, before the formation of the shear failure crack, another shear crack arose but it did not degenerate in a shear failure crack once it was crossed by the intermediate sheet strip (see Fig. 11d and scheme inset of Fig. 20). Due to the fact that this crack has crossed this sheet strip near  $SG_{CV8}$  (Fig. 20), the largest strain increment after the formation of this crack was observed in this strain gauge. With the widening process of this crack the resisting bond length of this sheet strip was mobilized, resulting in a significant strain increment on the  $SG_{CV8}$  strain gauge. Since the resisting bond length of this sheet strip avoided the degeneration of this shear crack into a shear failure crack, another shear crack formed in between the two sheet strips closest to the loaded section. When this shear crack crossed the intermediate



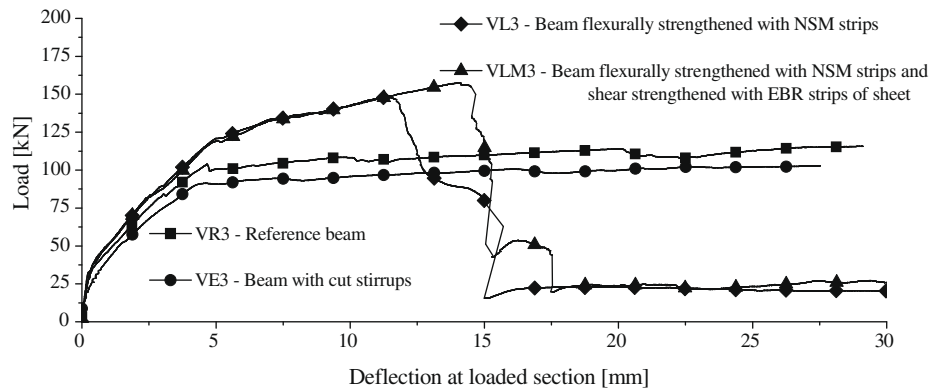


Fig. 19. Deflection-load relationship for the beams of Series 3.

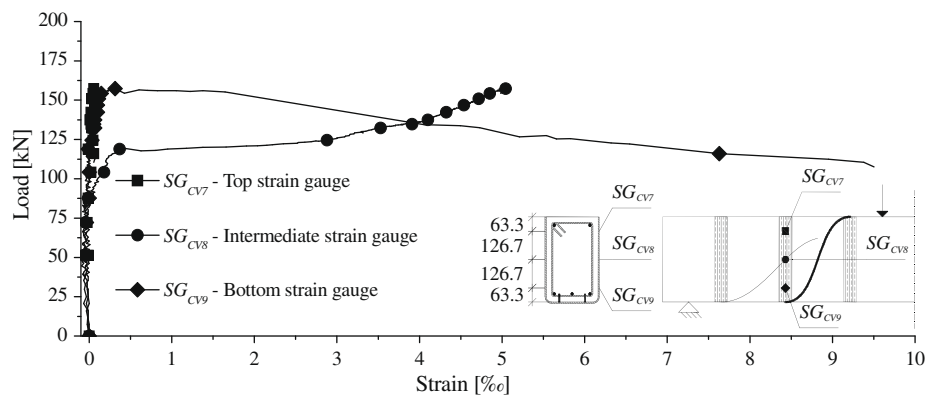


Fig. 20. Relationship between the strains in the EBR strip of sheet ( $SG_{CV7}$ ,  $SG_{CV8}$ ,  $SG_{CV9}$ ) and the applied load, in VLM3 beam (dimensions in mm).

sheet strip at its bottom part, an abrupt increase of strain was registered in  $SG_{CV9}$ .

## 5. Conclusions

In this work, an experimental program was carried out to assess potential changes in the load carrying capacity of RC beams when steel stirrups are cut to install CFRP strips for the flexural strengthening of the beams according to the NSM technique. For this purpose, three series of RC beams, each one composed of four beams, were tested. From the obtained results, the following conclusions can be made:

- For beams subject to an increasing monotonic loading, and with a percentage of steel stirrups higher than the minimum one, cutting the bottom arm of the steel stirrups for the installation of CFRP strips led to a decrease in beam load carrying capacity of less than 10%, when the corresponding reference beam (with intact steel stirrups) was considered for comparison purposes.
- In RC beams with a longitudinal steel reinforcement ratio of about 0.4%, which is significantly higher than the minimum percentage, an increment of the beam's load carrying capacity larger than 50% can be obtained by applying CFRP strips according to the NSM technique, even in beams with the bottom arm of the steel stirrups cut for the installation of these strips. However, this strengthening performance can only be attained if the shear failure of the beam and the premature detachment of the concrete cover that includes the CFRP strips are avoided. These both types of failure modes can be avoided applying U or O (full wrapping) shear strengthening configurations composed

by strips of CFRP wet lay-up sheet, according to the EBR technique, in a percentage and with strip spacing recommended by fib or ACI guidelines.

- The influence of cyclic and fatigue loadings on the strengthening effectiveness of RC beams with cut steel stirrups for the installation of NSM CFRP strips needs to be addressed by specific research programs.

## Acknowledgements

The study reported in this paper forms a part of the research program "CUTINEMO" supported by FCT, PTDC/ECM/73099/2006. The authors wish to acknowledge the support also provided by the Casais, S&P, SECIL and Artecanter Companies. The first Author acknowledges the grant under the aforementioned research project.

## References

- [1] ACI Committee 440 – guide for the design and construction of externally bonded FRP systems for strengthening concrete structures. American Concrete Institute; 2007. 118 p.
- [2] Barros JAO, Kfotynia, R. Possibilities and challenges of NSM for the flexural strengthening of RC structures. In: Fourth international conference on FRP composites in civil engineering (CICE2008), Zurich, Switzerland; 22–24 July 2008.
- [3] Barros JAO, Dias SJE, Lima JLT. Efficacy of CFRP-based techniques for the flexural and shear strengthening of concrete beams. *J Cem Concr Compos* 2007;29(3):203–17.
- [4] De Lorenzis L, Nanni A. Shear strengthening of reinforced concrete beams with near-surface mounted fiber-reinforced polymer rods. *ACI Struct J* 2001;98(1):60–8.

- [5] Taljsten B. FRP strengthening of existing structures design guideline. Lulea University of Technology; 2006.
- [6] El-Hacha R, Rizkalla SH. Near-surface-mounted fiber-reinforced polymer reinforcements for flexural strengthening of concrete structures. *ACI Struct J* 2004;101(5):717–26.
- [7] Bianco V, Barros JAO, Monti G. Bond model of NSM - CFRP in the context of the shear strengthening of RC beams. *ASCE J Struct Eng* 2009;135(6): 619–31.
- [8] Barros JAO, Fortes AS. Flexural strengthening of concrete beams with CFRP laminates bonded into slits. *J Cem Concr Compos* 2005;27(4):471–80.
- [9] Bonaldo E, Barros JAO, Lourenço PJB. Efficient strengthening technique to increase the flexural resistance of existing RC slabs. *J Compos Construct* 2008;12(2):149–59.
- [10] Dias SJE, Barros JAO. Shear strengthening of T cross section reinforced concrete beams by near surface mounted technique. *J Compos Construct* 2008;12(3): 300–11.
- [11] Haskett MH, Oehlers DJ, Wu C. Improved IC debonding resistance of embedded NSM FRP plates. In: Asia-Pacific conference on FRP in structures; APFIS 2007.
- [12] Fib – Bulletin 14. 2001. Externally bonded FRP reinforcement for RC structures. Technical report by Task Group 9.3 FRP, 130.
- [13] Lima JLT, Barros, JAO. Design models for shear strengthening of reinforced concrete beams with externally bonded FRP composites: a statistical vs reliability approach. FRPRCS-8. University of Patras; July 16–18, 2007.
- [14] Costa IG. The influence of cutting the steel stirrups for the installation of CFRP NSM laminates for the flexural strengthening of RC beams. Department of Civil Engineering; June 2008 [in Portuguese].